



HAL
open science

Photoinduced Arylation of Acridinium Salts: Tunable Photoredox Catalysts for C-O Bond Cleavage

Yi-Xuan Cao, Gan Zhu, Yiqun Li, Nolwenn Le Breton, Christophe Gourlaouen, Sylvie Choua, Julien Boixel, Henri-Pierre Jacquot de Rouville, Jean-François Soulé

► **To cite this version:**

Yi-Xuan Cao, Gan Zhu, Yiqun Li, Nolwenn Le Breton, Christophe Gourlaouen, et al.. Photoinduced Arylation of Acridinium Salts: Tunable Photoredox Catalysts for C-O Bond Cleavage. *Journal of the American Chemical Society*, 2022, 144 (13), pp.5902-5909. 10.1021/jacs.1c12961 . hal-03632077

HAL Id: hal-03632077

<https://hal.science/hal-03632077>

Submitted on 27 Apr 2022

HAL is a multi-disciplinary open access archive for the deposit and dissemination of scientific research documents, whether they are published or not. The documents may come from teaching and research institutions in France or abroad, or from public or private research centers.

L'archive ouverte pluridisciplinaire **HAL**, est destinée au dépôt et à la diffusion de documents scientifiques de niveau recherche, publiés ou non, émanant des établissements d'enseignement et de recherche français ou étrangers, des laboratoires publics ou privés.

Photoinduced Arylation of Acridinium Salts: Tunable Photoredox Catalysts for C–O Bond Cleavage

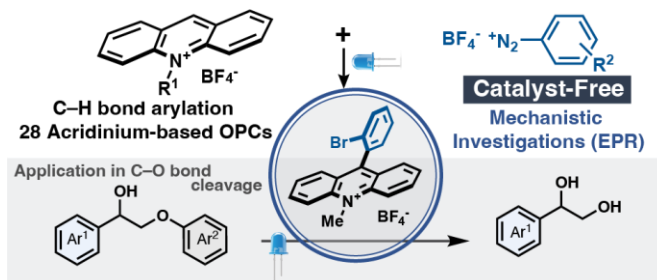
Yi-Xuan Cao,^{‡,‡} Gan Zhu,^{‡,¶,‡} Yiqun Li,[¶] Nolwenn Le Breton,[§] Christophe Gourlaouen,[§] Sylvie Choua,^{‡,*} Julien Boixel,^{‡,*} Henri-Pierre Jacquot de Rouville^{§,*} and Jean-François Soulié^{‡,*}

[‡] Univ Rennes, CNRS UMR6226, F-3500 Rennes, France. [¶] Department of Chemistry, Jinan University, Guangzhou 511443. [§]Institut de Chimie de Strasbourg, CNRS UMR 7177, Université de Strasbourg, 4 rue Blaise Pascal, 67000 Strasbourg (France). ^{*}These authors contributed equally to this work.

KEYWORDS. Photoredox Catalysis – C–H Bond Arylation – C–O Bond Cleavage – Radicals

ABSTRACT: A photo-induced arylation of *N*-substituted acridinium salts has been developed and has exhibited a high functional group tolerance (e.g., halogen, nitrile, ketone, ester, nitro). A broad range of well-decorated C9-arylated acridinium catalysts with fine-tuned photophysical and photochemical properties, namely, excited-state lifetimes and redox potentials have been synthesized in a one-step procedure.

These functionalized acridinium salts were later evaluated in the photoredox-catalyzed fragmentation of 1,2-diol derivatives (lignin models). Among them, 2-bromophenyl substituted *N*-methyl acridinium has outperformed all photoredox catalysts, including commercial Fukuzumi's catalyst, for the selective C^βO–Ar bond cleavage of diol monoarylethers to afford 1,2-diols in good yields.



INTRODUCTION

Over the past decades, the development of photoredox catalysts (PCs) has revolutionized the way that chemists approach new chemical transformations. Indeed, light offers advantages of simple, cheap energy source allowing the production of highly reactive (radical) intermediates under mild conditions.^[1] Among PCs, acridinium-based molecules are used as strong oxidizing organic photoredox catalysts (OPCs), in which their photophysical and electrochemical properties can be modulated by incorporating functional group(s) at diverse positions.^[2] Since the development of Fukuzumi's catalyst (aryl = mesityl, Figure 1A),^[3] several Fukuzumi's congeners with tuned photoredox properties (E_{Red}^* up to 2.26 V vs SCE) were studied by pioneer research groups.^[4] This molecular diversity enables acridinium-dyes to be complementary or be even competitive with polypyridyl transition metal photoredox catalysts.^[1h] However, their design is still highly limited since the preparation of acridinium derivatives bearing sensitive functional groups (esters, ketones, nitriles, halogens) is often

prevented on account of the use of organometallic intermediates (Figure 1A, left).^{[4i]-[4m]} An alternative would be the photo-synthesis of acridinium derivatives from unfunctionalized acridinium cores *via* a radical C–H bond arylation (Figure 1A, right).^[5] In theory, a wide library of acridinium-OPCs could be directly accessed in one step due to high functional group tolerance of the radical pathway. The acridinium core is also a suitable aryl radical acceptor and its LUMO presents a major contribution at the C₉ position thus ensuring its regioselective functionalization.^[6] The elaboration of a new library of acridinium-OPCs offering a variety of E_{Red}^* should pave the way to the discovery of new photocatalyzed reactions.

The valorization of lignins under sustainable conditions provides greener opportunities for industry and academia to produce aromatic building blocks out of bio-sources.^[7] Especially, the visible-light-driven fragmentation of C–O bonds has gained an increasing interest and meets the requirements of sustainability (Figure 1B). The photocleavage of C–O bonds in lignin β -O-4 model compounds was recently reported in the presence of photoredox catalysis, iridium-based catalysts or OPCs, requiring the pre-oxidation of the benzylic alcohols.^[8] In these cases, the C(sp³)-O bond is cleaved affording acetophenone and phenol derivatives. In 2019, König and co-workers employed dual catalysis composed of 4CzIPN [1,2,3,5-tetrakis(carbazol-9-yl)-4,6-dicyanobenzene] as OPC and a thiol as hydrogen atom transfer catalyst for the neutral redox fragmentation of β -O-4 model compounds into acetophenone and phenol derivatives without pre-oxidation.^[9] In contrast, catalytic systems able to generate diols *via* formal C ^{β} O–Ar bond fragmentation of lignin models were barely described.^[10] We envisioned that using acridinium-OPC with a high excited-state reduction potential might induce the C ^{β} O–Ar bond fragmentation through the single electron oxidation of the phenolic unit of 1,2-diol monoarylethers—when Ar² is electron-richer than Ar¹ (Figure 1C).

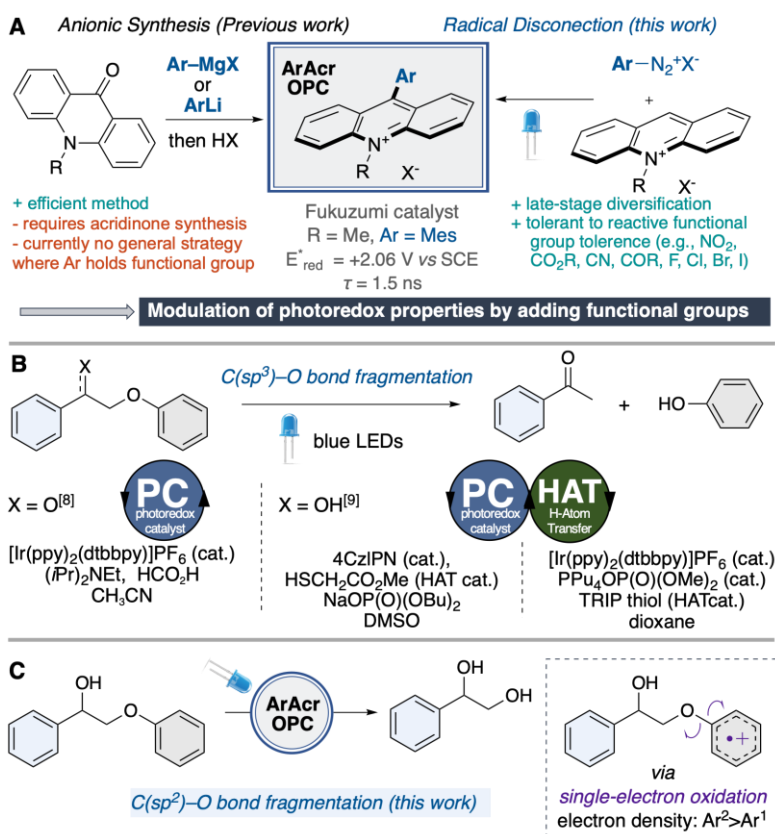


Figure 1. A) Synthetic routes for acridinium-based OPCs. B) Previous approaches for the photoinduced C–O bond fragmentation of 1,2-diol monoarylethers. C) Photoinduced C–O bond fragmentation of 1,2-diol monoarylethers *via* Single-Electron Oxidation.

Motivated by these challenges, we contemplated the possibility of preparing a wide library of acridinium-based OPCs bearing various substituents on the C9-aryl group. Our approach is based on radical C–H bond arylation from unfunctionalized *N*-methyl and *N*-aryl acridinium cores using aryldiazonium salts as radical precursors under blue light. The photosynthesis and the mechanistic study of a library of 28 acridinium-based OPCs is reported. Besides, the photophysical properties of 13 novel structures were studied in order to determine the best OPC candidate in the photoinduced C–O bond fragmentation of β -O-4 lignin models.

RESULT AND DISCUSSION

Synthesis of functionalized acridinium-based OPCs. *N*-methyl acridinium tetrafluoroborate (MeAcrH·BF₄) and 4-methoxyphenyl diazonium salt were selected as model substrates.^[11] Firstly, the reaction was performed in the presence of 2.5 mol% of Ru(bpy)₃Cl₂ as photoredox catalyst in CH₃OH under visible-light irradiation (blue LEDs).^[12] Under these conditions, the aryl radical was generated allowing the C–H bond arylation of acridinium salt at the C9-position affording **1** in 80% yield (Table 1, entry 1). Surprisingly, when the reaction is performed without Ru(bpy)₃Cl₂, the desired arylated acridinium **1** is obtained in 60% yield (Table 1, entry 2). A screening of solvents revealed that the reaction proceeded in higher yield in DMSO or in a mixture of CH₃OH/DMSO in 1:2 ratio (Table 1, entries 2-9). Control experiments demonstrated that the photo-reaction was less efficient with white light excitation and does not occur in the dark or in the presence of oxygen (Table 1, entries 10-12).

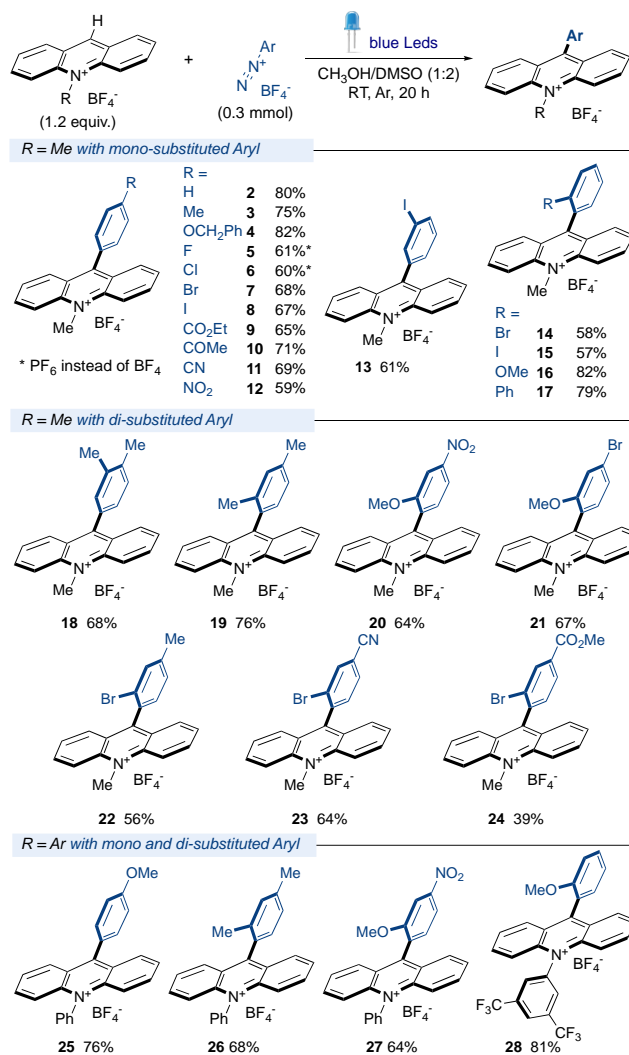
Table 1. Optimization of Photoinduced C9-H Bond Arylation of *N*-Methylacridinium (MeAcrH·BF₄).



Entry	Solvent	Yield of 1 (%) ^[a]
1 ^[b]	CH ₃ OH	80
2	CH ₃ OH	60
3	H ₂ O	-
4	Toluene	-
5	CH ₃ CN	55
6	DMSO	80
7	CH ₃ OH/CH ₃ CN (1:1)	50
8	CH ₃ OH/DMSO (1:2)	90
9	CH ₃ OH/DMSO (1:2)	95 (85)
10 ^[c]	CH ₃ OH/DMSO (1:1)	70
11 ^[d]	CH ₃ OH/DMSO (1:1)	-
12 ^[e]	CH ₃ OH/DMSO (1:1)	-

[a] The yields are determined by ¹H NMR using 1,2,3,4-tetrachloroethane as internal standard, isolated yield is shown in parentheses. [b] 2.5 mol% Ru(bpy)₃Cl₂. [c] white light. [d] dark. [e] O₂ atmosphere (P = 1 atm).

We then turned our attention to the scope of the reaction (Scheme 1). Unsubstituted phenyl aryldiazonium tetrafluoroborate smoothly reacted to afford the 9-phenyl *N*-methyl acridinium salts **2**, a commonly used OPC for alcohol oxidations,^[6a] in 80% yield. The reactivity of a set of *para*-substituted aryldiazonium tetrafluoroborate salts was evaluated from electron-rich groups (4-tolyldiazonium or 4-benzyloxy) to electron-withdrawing groups (ester, acetyl nitrile, nitro, etc.). All substrates **3-12** were obtained in reasonably good yields between 82-59% yields. Notably, in compound **4**, the benzyloxy unit remains untouched and could be further deprotected to afford the corresponding hydroxyphenyl group with potential application in ultrafast photoinduced charge transfer reaction.^[13] It should be mentioned that 9-arylacridinium as hexaphosphate (PF₆) salts have been also prepared.^[14] In contrast to the previous synthetic methods employing organometallics, this radical procedure also allowed the introduction of *para*-halogenated phenyl ring (i.e., X = F, Cl, Br, I), and *meta*-iodo-phenyl ring, suitable functional group for further transformation. The 9-aryl-*N*-methyl acridinium salts **14-17**, bearing bromo-, iodo-, methoxy-, phenyl group at *ortho*-position of the C₉-aryl ring were obtained in good yields. In addition, disubstituted aryldiazonium salts also underwent photoinduced C–H bond arylation of *N*-methyl acridinium nicely (**18**, 68%) even for the formation of *ortho*-functionalized derivatives with a methyl (**19**, 76%), a methoxy (**20-21**, 64% and 67%). A set of acridinium containing a 4-substituted-2-bromophenyl at the C9 position was also prepared (**22-24**, 39% < yield < 64%).^[15]



Scheme 1. Scope of Photoinduced-C9-Arylation of *N*-Methyl or *N*-Aryl Acridinium Salts with Aryl diazonium Salts.

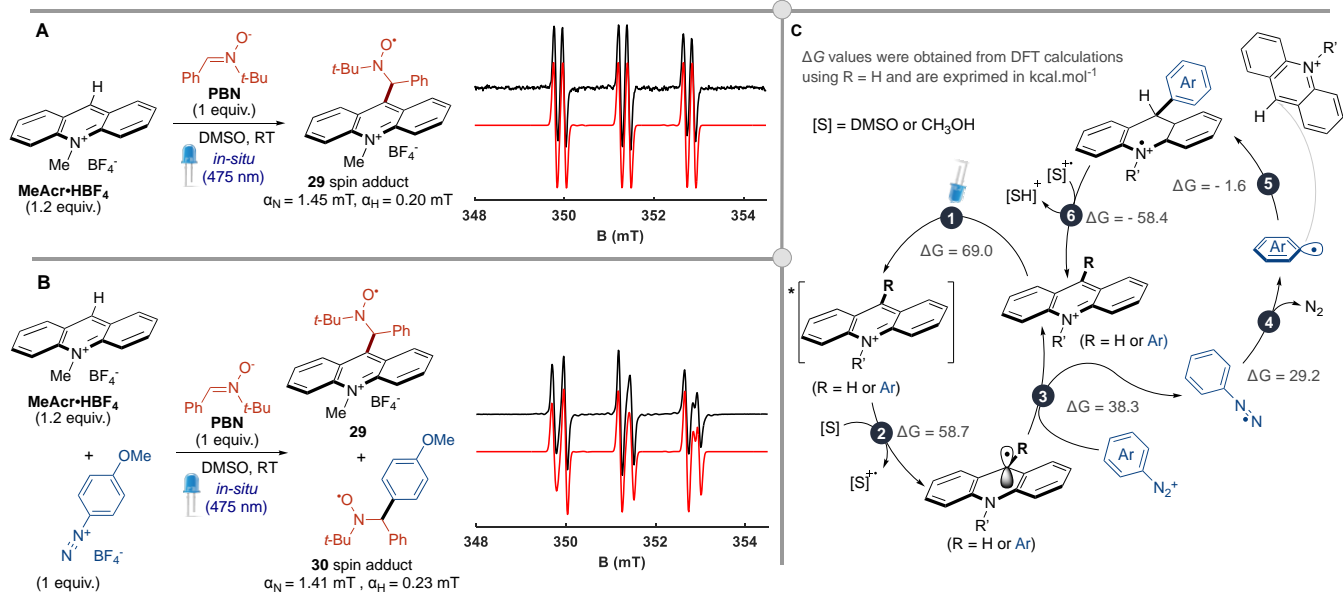
Under these conditions, *N*-phenyl acridinium was also arylated at the C9 position affording the functional 9-aryl-*N*-phenyl acridinium salts **25-27** in good yields. The photoinduced coupling between electron-deficient *N*-(3,5-bis(trifluoromethyl)phenyl)acridinium and 2-methoxybenzenediazonium salts led to the formation of push-pull system **28** in 81% yield.

Mechanistic Study. Then, we conducted mechanistic investigations to understand the formation of **1** without photoredox catalyst (Figure 2). When the reaction was performed without light irradiation at 65 °C, no formation of **1** was detected suggesting that no thermal activation of the diazonium salts occurred (see ESI, Figure S1).^[16] This result indicates that MeAcrH·BF₄ unambiguously acts as a photosensitizer in the generation of the aryl radical. This hypothesis was further supported by radical quenching experiments, in which the reaction was prevented in the presence of TEMPO [= (2,2,6,6-tetramethylpiperidin-1-yl)oxyl, 2 equiv.] (see ESI, Figure S2). Next, UV/visible spectroscopy experiments confirmed that the reaction between MeAcrH·BF₄ and 4-methoxyphenyl diazonium salts did not generate an EDA [=electron donor-acceptor]^[17] association complex (see ESI, Figure S4). Electron Paramagnetic Resonance spectroscopy (EPR)-Spin Trap-

ping was essential for probing transient radical species using *N*-tert-butyl- α -phenylnitron (PBN).^[18] In a 1:1 mixture of MeAcrH·BF₄ and PBN in DMSO under blue light irradiation, a spin-adduct attributed to the acridinyl **29** was formed. The obtained EPR spectrum was consistent with an adduct formed from α -C-centered radical with hyperfine coupling constants (*hfccs*) of $\alpha_N = 1.45$ mT and $\alpha_H = 0.20$ mT (Figure 2A). By contrast, when mixing MeAcrH·BF₄, 4-methoxybenzenediazonium tetrafluoroborate and PBN under the same conditions, the EPR spectrum shows a mixture of spin-adducts formed by the trapping of two different C-centered radicals (Figure 2B). The experimental spectrum was analyzed by means of a computer simulation suggesting the presence of the acridinyl (**29**, $\alpha_N = 1.45$ mT and $\alpha_H = 0.20$ mT) and phenyl spin trap adducts (**30**, $\alpha_N = 1.41$ mT and $\alpha_H = 0.23$ mT) in a 3:7 ratio after 3 minutes of irradiation.^[19]

Based on the above results, a reaction pathway was proposed (Figure 2C). Upon irradiation of the MeAcrH·BF₄ (*step 1*), generation of the reduced acridinyl radical was achieved by mediation of a solvent molecule (*step 2*). A similar formation of an acridinyl radical had been previously reported by Kano and co-workers from photoexcited acridinium moieties.^[20] This hypothesis was further corroborated by DFT calculations showing the exergonic electron transfer from the solvent to the excited acridinium salt (10.3 kcal mol⁻¹). All used diazonium salts were then efficiently reduced by the acridinyl radical as clearly evidenced by EPR experiments (*step 3* and Figure 2A).^[21] These results are in agreement with a thermodynamically favored electron transfer (-0.2 V < $E_{1/2}(\text{diazonium/aryl radical})$ < $+0.2$ V vs SCE,^[22] $E_{1/2}(\text{acridinium/acridinyl radical}) = -0.54$ V vs SCE^[6a]) and the formation of an aryl radical (*step 4*). The aryl radical further reacted with the regenerated acridinium precursor leading to the corresponding acridane species (*step 5*). It is worthwhile to note that this species was not monitored by EPR experiments suggesting a short lifetime. Its reoxidation into the final product was further supported by DFT calculations (*step 6*, $\Delta G = -58.4$ kcal mol⁻¹). Finally, EPR control experiments evidenced the photocatalytic activity of **1** acting as acridinium photocatalyst for the generation of **29** (see ESI, Figure S10). This observation is in good agreement the high yields observed for the formation of the various Fukuzumi congeners (**1-19**) resulting in a constant concentration photocatalysts in the reaction mixture.^[23]

Figure 2. **A)** Spin trap experiment between MeAcrH·BF₄ and PBN. **B)** Spin trap experiment between MeAcrH·BF₄, 4-methoxyphenyl diazonium salts and PBN (in black-line are the experimental ERP data, in red-line are the simulation). **C)** Proposed mechanism for the Photoinduced-C9-Arylation of *N*-Methyl Acridinium Salts with Aryl diazonium Salts.



Photophysical properties of functionalized acridinium-based OPCs. The photophysical and electrochemical properties of the novel C₉-aryl *N*-methyl and *N*-aryl acridinium prepared by this photoinduced C–H bond arylation were examined (Table 2, and Figures S10-22).

Electronic absorption. The electronic absorption spectra of the newly synthesized acridinium salts, recorded in CH₃CN solution ($c \approx 10^{-5}$ M, 298 K), are presented in Figure 3 (left), and the related data are summarized in Table 2. All spectra are composed of three sets of absorption bands, two in the U.V. region (250-270 nm and 330-370 nm) and one in the visible part (from 400 to 550 nm). Except for **4** and **25**, all acridinium salts exhibit similar structured absorption spectra profiles in the visible region, indicating that the various structural modifications do not affect the ground state electronic properties. Compounds **4** and **25**, bearing a *para*-*O*-alkyl group on the 9-aryl, present a bathochromic and structureless absorption in the visible region, which is attributed to additional charge transfer from the *O*-alkyl phenyl group to the *N*-acridinium part.^[24] The acridinium **28** shows a red-shifted visible absorption band ($\lambda \approx 25$ nm) compared to its congeners. This shift is attributed to the combination of an *O*-alkyl substituent, in *ortho*-position of the C₉-aryl, and an electron-withdrawing *N*-phenyl(CF₃)₂ group.

Emission spectroscopy. The emission intensities and profiles of the novel acridinium salts are mainly dependent on the structure and electronic nature of the C₉-aryl group. Photophysical studies have revealed that depending on the nature of the C₉-aryl group, the first singlet state is either localized on the acridinium core (LEs)^[3, 25] or involves an intramolecular charge transfer from the C₉-aryl group to the acridinium core (CTs).^[4a, 26] In general, the C.T. state is favored upon increasing the electron donating character of the aryl group and upon functionalization at the 2'-position.^[27] Experimentally, both excited states have been observed along the present acridinium series. Figure 3 (middle and right) shows the emission spectra of salts **4** to **28** in CH₃CN solution. Acridiniums **7**, **10**, **14**, **17**, **18**, **23**, **24**, **26**, and **27** exhibit structured emission bands, characteristic of locally excited state (LEs) with large differences in photoluminescence quantum yields (Φ_{em}). It is worthwhile to note that the *ortho*-functionalized acridinium with a bromine atom (**14**, **23**, and **24**) exhibits the highest

Φ_{em} with identical energies ($\lambda_{max} = 514$ nm, $\Phi_{em} \approx 0.8$) as the result of less non-radiative deactivation pathways. Compared to **14**, no alteration of the emission energies was observed in the presence of an electron-withdrawing group at the 4'-position in **23** and **24** (nitrile and acetyl, respectively). These observations can be related to the forced orthogonal geometry between the C₉-aryl group and the acridinium core imposed by the Br atom thus breaking all electronic communication. In line with the above comments, the intense luminescence ($\Phi_{em} \approx 0.7$) and the identical emission energies of **26** and **27** were assigned to a restricted free rotation on C₉-position induced by the methyl and the methoxy substituent, respectively. In contrast, the free rotation of the C₉-aryl group allowed in compounds **7**, **10** and **18**, opens additional deactivation pathways and lowers the luminescence intensity (Φ_{em} c.a. 0.1 -0.2). For **17**, while a phenyl ring is present in the 2'-position, its free rotation lowers the photoluminescence quantum yields ($\Phi_{em} = 0.24$). The weak luminescence of compound **15** ($\Phi_{em} < 0.02$) was attributed to the presence of the iodine atom (at the 2'-position) favoring a radiationless intersystem crossing process (singlet to triplet excited state quenching *via* spin-orbit coupling). Acridiniums **4** and **25** display singlet charge transfer (CTs) emissive state with broad bands centered at 565 and 674 nm due to the presence of the electron-donating substituents at the 4'-positions, *i.e.* *O*-Me and *O*-benzyl, respectively. The push-pull feature of **27** induces an intense charge-transfer transition, leading to a lower-energy emissive state ($\lambda_{max} = 636$ nm) and a very weak luminescence ($\Phi_{em} = 0.008$). In accordance with less non-radiative deactivation pathways observed with a 2'-substitution, acridiniums **14**, **15**, **23**, **24**, **26**, and **27**, show relative long luminescence lifetimes of 10.0 to 19.2 ns well suited for bimolecular substrate activation and comparable to those of the most efficient acridinium photocatalysts.^[28]

Figure 3. Absorption (A) and Emission (B, C) Spectra of the Novel 9-Arylacridinium Salts in CH₂Cl₂ ($c = 10^{-5}$ M) at 298 K

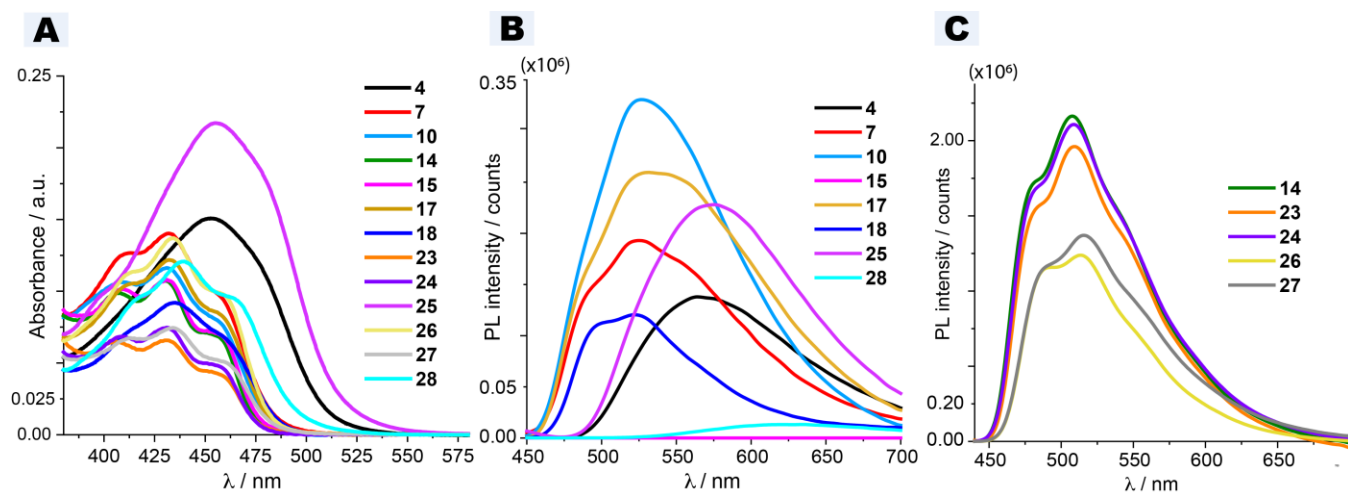


Table 2. Photophysical Properties of the Novel 9-Arylacridinium Salts

<i>N</i>	9-Ar	$E_{0,0}^a$	$E_{1/2}(C/C)^b$	$E_{1/2}(C^+/C)^c$	λ_{abs}^d [nm] ($\epsilon \times 10^3 [M^{-1}cm^{-1}]$)	λ_{em}^e [nm] ($\Phi_{em}[\%]$; τ^f [ns])
Substitution	Substitution	[eV]	[V vs SCE]	[V vs SCE]		

4	-CH ₃	4'-OBn	2.46	-0.58	1.88	264, 329, 345, 369, 453	565 (15; 6.4)
7	-CH ₃	4'-Br	2.61	-0.51	2.10	264, 331, 347, 363, 411, 431, 460	485, 523 (13; 1.3, 8.3)
10	-CH ₃	4'-COCH ₃	2.60	-0.49	2.11	264, 331, 346, 363, 407, 430, 458	486, 523 (23; 2.0, 14.3)
14	-CH ₃	2'-Br	2.65	-0.48	2.17	264, 331, 347, 364, 407, 430, 457	481, 507, 543sh (83; 16.9)
15	-CH ₃	2'-I	2.63	-0.48	2.15	264, 331, 348, 364, 410, 431, 459	507 (2; <2)
17	-CH ₃	2'-C ₆ H ₅	2.61	-0.52	2.09	264, 331, 347, 363, 412, 432, 459	487sh, 527 (24; 7.8)
18	-CH ₃	3',4'-(CH ₃) ₂	2.59	-0.56	2.03	263, 346, 360, 413, 435, 464	491, 524 (13, <2)
23	-CH ₃	2'-Br-4'-CN	2.64	-0.42	2.22	264, 334, 349, 366, 406, 430, 458	482, 508, 544sh (80; 19.2)
24	-CH ₃	2'-Br-4'-CO ₂ CH ₃	2.65	-0.44	2.21	264, 333, 349, 365, 409, 431, 458	481, 508, 545sh (82; 18.0)
25	-C ₆ H ₅	4'-OCH ₃	2.45	-0.52	1.93	266, 344, 361, 456	574 (20, 6.3)
26	-C ₆ H ₅	2',4'-(CH ₃) ₂	2.63	-0.51	2.12	265, 328, 345, 361, 412, 433, 462	491, 515 (65, 10.0)
27	-C ₆ H ₅	2'-OCH ₃ -4'-NO ₂	2.62	-0.43	2.19	265, 296, 334, 349, 364, 414, 434, 461	489, 515, 551sh (69; 12.0)
28	-C ₆ H ₃ (CF ₃) ₂	2'-OCH ₃	2.38	-0.42	1.96	267, 331, 347, 363, 415, 440, 468	636 (0.8, 6.4)

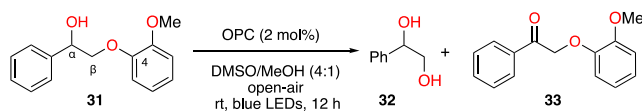
[a] determined at the intersection between normalized absorption and emission spectra, with $E = 1240/\lambda$. [b] Ground state reduction potentials determined by cyclic voltammetry (E vs. SCE). [c] Excited-state reduction potential, estimated with ground state reduction potentials and excited-state energies (see ESI for details). [d] conc. $\approx 1.5 \times 10^{-5}$ M. [e] $\lambda_{\text{ex}} = 370$ nm with ref = Quinine sulfate ($\Phi = 0.546$ in H₂SO₄ 0.5 M). [f] Time-correlated single-photon counting (TCSPC) technique, $\lambda_{\text{ex}} = 375$ nm

Electrochemistry. Cyclic voltammograms of all the prepared acridinium salts were recorded in CH₃CN solution and are presented in Figures S10-22, and the related potential are listed in Table 2. Except for **26**, they all exhibit two reduction waves. The first ground state reduction processes are reversible for all systems, with potentials ranging from -0.42 to -0.58 V vs SCE. As a rule of thumb, the introduction of electron-donating groups on the 4'-position of the C₉-aryl (**4**, **18**, **25**, **26**) leads to a cathodic shift of reduction potential, while electron-withdrawing substituents leads to an anodic shift of reduction potential (**10**, **23**, **24**, **27**). In consequence, the photoredox properties of the different catalysts ($E_{1/2}(\text{B}^*/\text{B}^-)$) were estimated to be comprise between $+1.88$ and $+2.22$ V vs SCE. The lowest excited-state potentials ($E_{1/2}(\text{B}^*/\text{B}^-) < 2.00$ V) were found for the acridiniums **4**, **25**, and **28** displaying CT excited-states. While the highest $E_{1/2}(\text{B}^*/\text{B}^-)$ were measured for catalysts bearing functionalization at the 2'-position (**14**, **15**, **23**, **24**, **27**) since free rotations are restricted between the acridinium core and its appended aromatic moiety.

Application of functionalized acridinium-based OPCs in Oxidative Cleavage of β -O-4 lignin models. Inspired by the pioneering work of Fukuzumi and his co-workers on the oxidation of benzyl alcohol using 9-phenyl-10-methylacridium as OPC,^[29] and by the recent C–O bond cleavage of diaryl ethers by acridinium photocatalysts,^[30] the fragmentation C ^{β} O–Ar bond induced by acridinium-based OPCs was investigated. The choice 2-(2-methoxyphenoxy)-1-phenylethan-1-ol (**31**) as model substrate was made since its phenolic unit is enriched by a methoxy-substituent thus facilitating its single electron-oxidation. The reaction was carried out in the presence of 2 mol% of OPC in DMSO/CH₃OH in a 4:1 mixing ratio in open air and blue LEDs irradiation for 12 h (Table 3). Fukuzumi's catalyst ($E_{\text{red}}^* = 2.06$ V vs SCE) proved to be inefficient for this transformation (Table 1, entry 1) affording only the ketone product **33** in trace amounts. 9-Phenyl-10-methylacridium (**2**) and OPCs **7** or **10** –exhibiting slightly higher excited state reduction potentials than Fukuzumi's catalyst ($E_{\text{red}}^* = 2.19$, 2.11 and 2.17 V vs. SCE)– were also ineffective (Table 1, entries 2-4). This lack of catalytic performance was attributed to a possible photobleaching arising from radical coupling reactions at the C9-position.^[28] This deactivation pathway could be prevented by the introduction of more hindered C9-aryl group. Indeed, when the reaction was carried out in the presence

of **14** ($E_{\text{red}}^* = 2.17$ V vs. SCE), bearing 2'-bromophenyl at the C9 position, the $\text{C}^\beta\text{O-Ar}$ bond cleavage occurred in high yield affording the diol **32** in 84% isolated yield. OPCs **15** and **17** ($E_{\text{red}}^* = 2.15$ and 2.09 V vs. SCE), bearing respectively 2'-iodophenyl, and 2'-biphenyl at the C9 position, displayed a lower reactivity than **14** resulting from their lower excited-state reduction potential and excited lifetime. Interestingly, reactions with OPCs possessing higher E_{red}^* values and longer excited lifetime, **23** and **24** ($E_{\text{red}}^* = 2.22$ and 2.21 V vs. SCE) led to **32** in 75% and 78% yield, respectively (Table 1, entries 8 and 9). Compared to **14**, their lower reactivity might be explained by their degradation during the C–O bond fragmentation. Indeed, nitrile and ester functional groups are prone to react with nucleophiles such as alcohols or other radicals. Finally, control experiments in the absence of catalyst or oxygen did not give rise to any conversions (Table 1, entries 10 and 11). One can notice that guaiacol was not detected after the reaction. It has been previously demonstrated that under photocatalytic oxidative conditions, phenol derivatives are not stable and quickly transform into complex mixtures.^[31] To corroborate this hypothesis, a control experiment was carried out with guaiacol as the substrate under the same reaction conditions. The result shows that most of the guaiacol was consumed during the reaction.

Table 3. Screening of OPC in Visible-Light Fragmentation

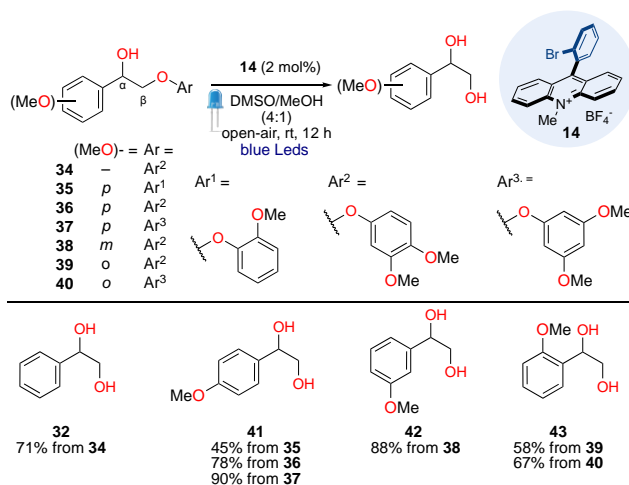


Entry	OPC	Conv. (%) ^[a]	32 (%) ^[a]	33 (%) ^[a]
1 ^[b]	Fukuzumi	25	0	5
2	2	12	0	0
3	7	0	–	0
4	10	0	–	0
5	14	100	89 (84)	0
6	15	80	47	0
7	17	72	41	0
8	23	78	75	0
9	24	80	78	0
10	–	0	0	0
11 ^[b]	14	0	0	0
12 ^[c]	14	0	0	0

[a] The conversion is based on **32** consumption and the yields are determined by GC-analysis using biphenyl as the internal standard. [b] Traces of overoxidized products (e.g., benzaldehyde and benzoic acid) Isolated yield is shown in parentheses. [b] Under argon atmosphere. [c] Using guaiacol instead of **31**.

Next, a Stern–Volmer quenching study was conducted to monitor the kinetic behavior of the photoexcited acridinium-catalyst **14** in the presence of **34**. Interestingly, the photoexcited state of **14** was readily quenched by **34** in degassed CH_2Cl_2 at room temperature (Figures S25-27). These observations suggest that the C–O bond cleavage occurs through electron transfer between [**14**]^{*} and diol monoarylethers (Single-Electron Oxidation) as proposed in the Figure1B.^[32]

The scope of the photo-oxidative catalytic reaction was probed using the best OPC, namely **14**, on various Lignin models (Scheme 2). Firstly, the methoxy substitution pattern of the phenolic part (Ar^1 - Ar^3) was varied in order to represent the different units present in native lignin (coumaryl, coniferyl, and sinapyl alcohols). First, the selective $\text{C}^\beta\text{O}-\text{Ar}$ bond cleavage of 2-(3,5-dimethoxyphenoxy)-1-phenylethanol (**34**) afforded **32** in 71% yield. When using 2-(2-methoxyphenoxy)-1-(4-methoxyphenyl)ethan-1-ol (**35**) in which both arene rings display similar electronic properties, the photocatalytic C–O bond cleavage led to the 1-(4-methoxyphenyl)ethane-1,2-diol (**41**) in a moderate 45% yield. However, when the phenolic part contains two methoxy groups, such as in **36** or **37**, the diol **42** was isolated in better 78% and 90% yields. From 2-(3,4-dimethoxyphenoxy)-1-(3-methoxyphenyl)ethan-1-ol (**38**), the diol **42** was obtained by selective C–O bond cleavage in 88% yield. Finally, 1-(2-methoxyphenoxy)ethane-1,2-diol (**43**) was isolated in 51% or 67% yield, respectively from **39** and **40**.



Scheme 2. Scope of $\text{C}^\beta\text{O}-\text{Ar}$ Lignin Model Substrates in Photocatalytic C–O Bond Fragmentation.

CONCLUSION

We have developed a late-stage diversification of acridinium salts involving a radical-based regioselective $\text{C}_9\text{-H}$ bond arylation using aryl diazonium salts, affording a library of well-decorated fluorophores in only one step. The C–C bond formation under catalyst-free conditions involves a cross-coupling of aryl radicals, arising from a photoinduced electron transfer from aryl diazonium salt to the singlet excited state of *N*-methyl or aryl acridinium salts, as demonstrated by EPR spin-trap experiments. Owing to the mild reaction conditions, a particularly broad scope was established, encompassing sensitive products containing nitrile, nitro, ester, ketyl, and halogen functional groups. The impact of the nature of the C_9 -aryl group on the photoredox properties was also studied in detail. As a general trend, the introduction of an electron-donating group (alkoxide or alkyl group) lowered the excited state reduction potentials, while the acridinium holding a C_9 -aryl group with an electron-withdrawing group (NO_2 , nitrile, ester, ketyl, halo) displayed higher excited state reduction potentials than the parent Fukuzumi catalyst. The introduction of only one bulky group, such as bromo, at the 2'-position, is sufficient to improve the quantum yield and the excited live time due to an orthogonal orientation of the Ar and Acr^+ moieties. This streamline has allowed designing a novel organic photoredox for the $\text{C}^\beta\text{O}-\text{Ar}$ fragmentation of diol monoarylethers to afford 1,2-diols in good yields that constitutes a vital step toward converting lignin to value-added low-molecular-weight aromatics. Current efforts to understand and extend this process to native lignin are underway.

ASSOCIATED CONTENT

Supporting Information

The Supporting Information is available free of charge on the ACS Publications website.

Detailed experimental procedures, characterization, additional mechanistic experiments, experimental decays, cyclic voltammograms UV-visible absorption and emission spectra for all new acridinium compounds and spectral data for all new compounds; (PDF).

AUTHOR INFORMATION

Corresponding Author

Julien Boixel – Univ Rennes, CNRS UMR6226, Rennes F-3500, France orcid.org/0000-0001-8704-8776 Email: julien.boixel@univ-rennes1.fr

Henri-Pierre Jacquot de Rouville – Institut de Chimie de Strasbourg, CNRS UMR 7177, Université de Strasbourg, 4 rue Blaise Pascal, 67000 Strasbourg (France) orcid.org/0000-0002-9508-6446 Email : hpjacquot@unistra.fr

Jean-François Soulé – Univ Rennes, CNRS UMR6226, Rennes F-3500, France ; orcid.org/0000-0002-6593-1995, Email : jean-francois.soule@univ-rennes1.fr

Authors

Yi-Xuan Cao – Univ Rennes, CNRS UMR6226, Rennes F-3500, France

Gan Zhu – Univ Rennes, CNRS UMR6226, Rennes F-3500, France & Department of Chemistry, Jinan University, Guangzhou 511443, China

Yiqun Li – Department of Chemistry, Jinan University, Guangzhou 511443, China orcid.org/0000-0002-3303-1730

Nolwenn Le Breton – Institut de Chimie de Strasbourg, CNRS UMR 7177, Université de Strasbourg, 4 rue Blaise Pascal, 67000 Strasbourg (France) orcid.org/0000-0002-5638-9444

Christophe Gourlaouen – Institut de Chimie de Strasbourg, CNRS UMR 7177, Université de Strasbourg, 4 rue Blaise Pascal, 67000 Strasbourg (France) orcid.org/0000-0002-2409-2849

Sylvie Choua – Institut de Chimie de Strasbourg, CNRS UMR 7177, Université de Strasbourg, 4 rue Blaise Pascal, 67000 Strasbourg (France) orcid.org/0000-0003-1005-3555,

Author Contributions

‡These authors contributed equally.

ACKNOWLEDGMENT

We are grateful to the "Jinan University short-term overseas research program" for a grant to G. Z. We thank CNRS, UR1 and "Rennes Metropole" for providing financial support.

REFERENCES

- (a) Balzani, V.; Juris, A., Photochemistry and Photophysics of Ru(II)-polypyridine Complexes in the Bologna group. From Early Studies to Recent Developments. *Coord. Chem. Rev.* **2001**, *211*, 97-115; (b) Yoon, T. P.; Ischay, M. A.; Du, J., Visible Light Photocatalysis as a Greener Approach to Photochemical Synthesis. *Nat. Chem.* **2010**, *2*, 527-532; (c) Prier, C. K.; Rankic, D. A.; MacMillan, D. W. C., Visible Light Photoredox Catalysis with Transition Metal Complexes: Applications in Organic Synthesis. *Chem. Rev.* **2013**, *113*, 5322-5363; (d) Levin, M. D.; Kim, S.; Toste, F. D., Photoredox Catalysis Unlocks Single-Electron Elementary Steps in Transition Metal Catalyzed Cross-Coupling. *ACS Cent. Sci.* **2016**, *2*, 293-301; (e) Plesniak, M. P.; Huang, H.-M.; Procter, D. J., Radical Cascade Reactions Triggered by Single Electron Transfer. *Nat. Rev. Chem.* **2017**, *1*, 0077; (f) Xie, J.; Jin, H.; Hashmi, A. S. K., The Recent Achievements of Redox-Neutral Radical C-C Cross-Coupling Enabled by Visible-Light. *Chem. Soc. Rev.* **2017**, *46*, 5193-5203; (g) Yi, H.; Zhang, G.; Wang, H.; Huang, Z.; Wang, J.; Singh, A. K.; Lei, A., Recent Advances in Radical C-H Activation/Radical Cross-Coupling. *Chem. Rev.* **2017**, *117*, 9016-9085; (h) Wang, C.-S.; Dixneuf, P. H.; Soulé, J.-F., Photoredox Catalysis for Building C-C Bonds from C(sp²)-H Bonds. *Chem. Rev.* **2018**, *118*, 7532-7585.
- (a) Fukuzumi, S.; Ohkubo, K., Selective Photocatalytic Reactions with Organic Photocatalysts. *Chem. Sci.* **2013**, *4*, 561-574; (b) Romero, N. A.; Nicewicz, D. A., Organic Photoredox Catalysis. *Chem. Rev.* **2016**, *116*, 10075-10166.
- Fukuzumi, S.; Kotani, H.; Ohkubo, K.; Ogo, S.; Tkachenko, N. V.; Lemmetyinen, H., Electron-Transfer State of 9-Mesityl-10-methylacridinium Ion with a Much Longer Lifetime and Higher Energy Than That of the Natural Photosynthetic Reaction Center. *J. Am. Chem. Soc.* **2004**, *126*, 1600-1601.
- (a) Lin, Y.-C.; Chen, C.-T., Acridinium Salt-Based Fluoride and Acetate Chromofluorescent Probes: Molecular Insights into Anion Selectivity Switching. *Org. Lett.* **2009**, *11*, 4858-4861; (b) Romero, N. A.; Margrey, K. A.; Tay, N. E.; Nicewicz, D. A., Site-selective Arene C-H Amination via Photoredox Catalysis. *Science* **2015**, *349*, 1326-1330; (c) Joshi-Pangu, A.; Lévesque, F.; Roth, H. G.; Oliver, S. F.; Campeau, L.-C.; Nicewicz, D.; DiRocco, D. A., Acridinium-Based Photocatalysts: A Sustainable Option in Photoredox Catalysis. *J. Org. Chem.* **2016**, *81*, 7244-7249; (d) Margrey, K. A.; McManus, J. B.; Bonazzi, S.; Zecri, F.; Nicewicz, D. A., Predictive Model for Site-Selective Aryl and Heteroaryl C-H Functionalization via Organic Photoredox Catalysis. *J. Am. Chem. Soc.* **2017**, *139*, 11288-11299; (e) Margrey, K. A.; Levens, A.; Nicewicz, D. A., Direct Aryl C-H Amination with Primary Amines Using Organic Photoredox Catalysis. *Angew. Chem. Int. Ed.* **2017**, *56*, 15644-15648; (f) McManus, J. B.; Nicewicz, D. A., Direct C-H Cyanation of Arenes via Organic Photoredox Catalysis. *J. Am. Chem. Soc.* **2017**, *139*, 2880-2883; (g) Tay, N. E. S.; Nicewicz, D. A., Cation Radical Accelerated Nucleophilic Aromatic Substitution via Organic Photoredox Catalysis. *J. Am. Chem. Soc.* **2017**, *139*, 16100-16104; (h) Eberhard, J.; Peuntinger, K.; Fröhlich, R.; Guldi, D. M.; Mattay, J., Synthesis and Properties of Acridine and Acridinium Dye Functionalized Bis(terpyridine) Ruthenium(II) Complexes. *Eur. J. Org. Chem.* **2018**, 2682-2700; (i) Fischer, C.; Sparr, C., Direct Transformation of Esters into Heterocyclic Fluorophores. *Angew. Chem. Int. Ed.* **2018**, *57*, 2436-2440; (j) Gini, A.; Uygur, M.; Rigotti, T.; Alemán, J.; García Mancheño, O., Novel Oxidative Ugi Reaction for the Synthesis of Highly Active, Visible-Light, Imide-Acridinium Organophotocatalysts. *Chem. Eur. J.* **2018**, *24*, 12509-12514; (k) Durka, K.; Urban, M.; Dąbrowski, M.; Jankowski, P.; Kliś, T.; Luliński, S., Cationic and Betaine-Type Boronated Acridinium Dyes: Synthesis, Characterization, and Photocatalytic Activity. *ACS Omega* **2019**, *4*, 2482-2492; (l) Fischer, C.; Kerzig, C.; Zilate, B.; Wenger, O. S.; Sparr, C., Modulation of Acridinium Organophotoredox Catalysts Guided by Photophysical Studies. *ACS Catal.* **2019**, 210-215; (m) White, A. R.; Wang, L.; Nicewicz, D. A., Synthesis and Characterization of Acridinium Dyes for Photoredox Catalysis. *Synlett* **2019**, *30*, 827-832; (n) MacKenzie, I. A.; Wang, L.; Onuska, N. P. R.; Williams, O. F.; Begam, K.; Moran, A. M.; Dunitz, B. D.; Nicewicz, D. A., Discovery and Characterization

- of an Acridine Radical Photoreductant. *Nature* **2020**, *580*, 76-80; (o) Yan, H.; Song, J.; Zhu, S.; Xu, H.-C., Synthesis of Acridinium Photocatalysts via Site-Selective C–H Alkylation. *CCS Chem.* **2021**, 317-325.
5. Fukuzumi, S.; Ohkubo, K.; Suenobu, T.; Kato, K.; Fujitsuka, M.; Ito, O., Photoalkylation of 10-Alkylacridinium Ion via a Charge-Shift Type of Photoinduced Electron Transfer Controlled by Solvent Polarity. *J. Am. Chem. Soc.* **2001**, *123*, 8459-8467.
6. (a) Koper, N. W.; Jonker, S. A.; Verhoeven, J. W.; van Dijk, C., Electrochemistry of the 9-Phenyl-10-Methylacridan/acridinium Redox System; a High-Potential NADH/NAD⁺ Analogue. *Recl. Trav. Chim. Pays-Bas* **1985**, *104*, 296-302; (b) Hu, J.; Ward, J. S.; Chaumont, A.; Rissanen, K.; Vincent, J.-M.; Heitz, V.; Jacquot de Rouville, H.-P., A Bis-Acridinium Macrocycle as Multi-Responsive Receptor and Selective Phase-Transfer Agent of Perylene. *Angew. Chem. Int. Ed.* **2020**, *59*, 23206-23212; (c) Jacquot de Rouville, H.-P.; Hu, J.; Heitz, V., N-Substituted Acridinium as a Multi-Responsive Recognition Unit in Supramolecular Chemistry. *ChemPlusChem* **2021**, *86*, 110-129.
7. Zakzeski, J.; Bruijninx, P. C. A.; Jongerius, A. L.; Weckhuysen, B. M., The Catalytic Valorization of Lignin for the Production of Renewable Chemicals. *Chem. Rev.* **2010**, *110*, 3552-3599.
8. (a) Kärkäs, M. D.; Bosque, I.; Matsuura, B. S.; Stephenson, C. R. J., Photocatalytic Oxidation of Lignin Model Systems by Merging Visible-Light Photoredox and Palladium Catalysis. *Org. Lett.* **2016**, *18*, 5166-5169; (b) Bosque, I.; Magallanes, G.; Rigoulet, M.; Kärkäs, M. D.; Stephenson, C. R. J., Redox Catalysis Facilitates Lignin Depolymerization. *ACS Cent. Sci.* **2017**, *3*, 621-628; (c) Luo, N.; Wang, M.; Li, H.; Zhang, J.; Liu, H.; Wang, F., Photocatalytic Oxidation–Hydrogenolysis of Lignin β-O-4 Models via a Dual Light Wavelength Switching Strategy. *ACS Catal.* **2016**, *6*, 7716-7721; (d) Luo, J.; Zhang, J., Aerobic Oxidation of Olefins and Lignin Model Compounds Using Photogenerated Phthalimide-N-oxyl Radical. *J. Org. Chem.* **2016**, *81*, 9131-9137; (e) Luo, J.; Zhang, X.; Lu, J.; Zhang, J., Fine Tuning the Redox Potentials of Carbazolic Porous Organic Frameworks for Visible-Light Photoredox Catalytic Degradation of Lignin β-O-4 Models. *ACS Catal.* **2017**, *7*, 5062-5070; (f) Yang, C.; Kärkäs, M. D.; Magallanes, G.; Chan, K.; Stephenson, C. R. J., Organocatalytic Approach to Photochemical Lignin Fragmentation. *Org. Lett.* **2020**, *22*, 8082-8085.
9. (a) Chen, K.; Schwarz, J.; Karl, T. A.; Chatterjee, A.; König, B., Visible Light Induced Redox Neutral Fragmentation of 1,2-Diol Derivatives. *Chem. Commun.* **2019**, *55*, 13144-13147; (b) Nguyen, S. T.; Murray, P. R. D.; Knowles, R. R., Light-Driven Depolymerization of Native Lignin Enabled by Proton-Coupled Electron Transfer. *ACS Catal.* **2020**, *10*, 800-805.
10. Zhu, C.; Ding, W.; Shen, T.; Tang, C.; Sun, C.; Xu, S.; Chen, Y.; Wu, J.; Ying, H., Metallo-Deuteroporphyrin as a Biomimetic Catalyst for the Catalytic Oxidation of Lignin to Aromatics. *ChemSusChem* **2015**, *8*, 1768-1778.
11. Both reagents have a tetrafluoroborate anion to avoid anion metathesis
12. (a) Xue, D.; Jia, Z.-H.; Zhao, C.-J.; Zhang, Y.-Y.; Wang, C.; Xiao, J., Direct Arylation of N-Heteroarenes with Aryldiazonium Salts by Photoredox Catalysis in Water. *Chem. Eur. J.* **2014**, *20*, 2960-2965; (b) Kalyani, D.; McMurtrey, K. B.; Neufeldt, S. R.; Sanford, M. S., Room-Temperature C–H Arylation: Merger of Pd-Catalyzed C–H Functionalization and Visible-Light Photocatalysis. *J. Am. Chem. Soc.* **2011**, *133*, 18566-18569.
13. Jones, G.; Farahat, M. S.; Greenfield, S. R.; Gosztola, D. J.; Wasielewski, M. R., Ultrafast Photoinduced Charge-Shift Reactions in Electron Donor-Acceptor 9-Arylacridinium Ions. *Chem. Phys. Lett.* **1994**, *229*, 40-46.
14. The reaction were performed from MeAcrH·PF₆ with areneArN₂·PF₆.
15. However, the reaction with 2,4,6-trimethylbenzenediazonium failed to afford the corresponding Fukuzumi structure. This lack of reactivity might be explained by the poor reactivity of *bis-ortho*-disubstituted aryl radical intermediates.
16. Gloor, B.; Kaul, B. L.; Zollinger, H., Decomposition of Aryldiazonium Ions in Homogenous Solutions Part II: Arylations with Benzenediazonium Ions and *p*-Nitrobenzenediazonium Ions in Dimethyl Sulfoxide. *Helv. Chim. Acta* **1972**, *55*, 1596-1610.
17. Lima, C. G. S.; de M. Lima, T.; Duarte, M.; Jurberg, I. D.; Paixão, M. W., Organic Synthesis Enabled by Light-Irradiation of EDA Complexes: Theoretical Background and Synthetic Applications. *ACS Catal.* **2016**, *6*, 1389-1407.

18. Halliwell, B.; Gutteridge, J. M. C., *Free Radicals in Biology and Medicine*. 5th ed.; Oxford University Press: Oxford U.K., 2015.
19. Spin quantification was performed according to a calibration curve obtained with TEMPO samples. The concentrations for the standard solutions prepared CH₃OH/DMSO (1:1) were 7.7 μ M, 38.6 μ M, and 77.2 μ M. The linear plot of the doubly integrated EPR signal of these TEMPO solutions versus the concentration was linear. It has been used to assess the spin concentration of the mixture MeArCH and PBN and the mixture of MeArCH, PNB and 4-methoxybenzenediazonium tetrafluoroborate. The results found are 0.4 μ M and 3.6 μ M, respectively. These results demonstrate that the reaction involves the formation of two radicals.
20. Kano, K.; Zhou, B.; Hashimoto, S., The Photoreduction Mechanism of 10-Methylacridinium Chloride in Methanol. The Formation of 9,10-Dihydro-9-methoxy-10-methylacridine and Hydride Transfer. *Bull. Chem. Soc. Jpn.* **1987**, *60*, 1041-1047.
21. Experiments carried out in the presence of sterically hindered diazonium salts, namely 2,6-dimethylbenzenediazonium and 2,6-dichlorobenzenediazonium did not lead to the formation of the desired product (see ESI, Figures S3-S6). Spin trap experiments coupled to mass spectrometry only revealed the presence of the spin trapped aryl radical showing a fast electron transfer.
22. Allongue, P.; Delamar, M.; Desbat, B.; Fagebaume, O.; Hitmi, R.; Pinson, J.; Savéant, J.-M., Covalent Modification of Carbon Surfaces by Aryl Radicals Generated from the Electrochemical Reduction of Diazonium Salts. *J. Am. Chem. Soc.* **1997**, *119*, 201-207.
23. DFT calculations have estimated similar Δ G values involving MeArCH and **1** as photocatalyst in the suggested mechanism.
24. Jonker, S. A.; Ariese, F.; Verhoeven, J. W., Cation Complexation with Functionalized 9-Arylacridinium ions: Possible Applications in the Development of Cation-Selective Optical Probes. *Red. Trav. Chim. Pays-Bas* **1989**, *108*, 109-115.
25. Benniston, A. C.; Harriman, A.; Li, P.; Rostron, J. P.; van Ramesdonk, H. J.; Groeneveld, M. M.; Zhang, H.; Verhoeven, J. W., Charge Shift and Triplet State Formation in the 9-Mesityl-10-methylacridinium Cation. *J. Am. Chem. Soc.* **2005**, *127*, 16054-16064.
26. Romero, N. A.; Nicewicz, D. A., Mechanistic Insight into the Photoredox Catalysis of Anti-Markovnikov Alkene Hydrofunctionalization Reactions. *J. Am. Chem. Soc.* **2014**, *136*, 17024-17035.
27. Tsudaka, T.; Kotani, H.; Ohkubo, K.; Nakagawa, T.; Tkachenko, N. V.; Lemmetyinen, H.; Fukuzumi, S., Photoinduced Electron Transfer in 9-Substituted 10-Methylacridinium Ions. *Chem. Eur. J.* **2017**, *23*, 1306-1317.
28. Vega-Peñalosa, A.; Mateos, J.; Companyó, X.; Escudero-Casao, M.; Dell'Amico, L., A Rational Approach to Organo-Photocatalysis: Novel Designs and Structure-Property Relationships. *Angew. Chem. Int. Ed.* **2021**, *60*, 1082-1097.
29. Ohkubo, K.; Suga, K.; Fukuzumi, S., Solvent-free Selective Photocatalytic Oxidation of Benzyl Alcohol to Benzaldehyde by Molecular Oxygen using 9-Phenyl-10-Methylacridinium. *Chem. Commun.* **2006**, 2018-2020.
30. Tan, F.-F.; He, X.-Y.; Tian, W.-F.; Li, Y., Visible-Light Photoredox-Catalyzed C–O Bond Cleavage of Diaryl Ethers by Acridinium Photocatalysts at Room Temperature. *Nat. Commun.* **2020**, *11*, 6126.
31. Chowdhury, P.; Nag, S.; Ray, A. K., Degradation of Phenolic Compounds through UV and Visible-Light-Driven Photocatalysis: Technical and Economic Aspects. In *Phenolic Compounds-Natural Sources, Importances, and Applications*, IntechOpen: London, UK, 2017; pp 395-417.
32. It is worthwhile to note that HRMS (ESI) analysis of the crude mixture after irradiation revealed the presence of the peak of the undegraded catalyst **14** after reaction with compound **34** demonstrating its photochemical stability under these conditions (Figure S29).